Fundamental experiments of axial-type BSCCO-bulk superconducting motor model

Muta, I; Jung, HJ; Hirata, T; Nakamura, T; Hoshino, T; Konishi, T

Fundamental Experiments of Axial-Type BSCCO-Bulk Superconducting Motor Model

I. Muta, H. J. Jung, T. Hirata, T. Nakamura, T. Hoshino and T. Konishi

Abstract— **An axial type HTS hysteresis motor has the same structure as a conventional axial flux type permanent magnet synchronous motor. The permanent magnet rotor of a conventional permanent magnet synchronous motor is replaced by a rotor made from HTS materials with the objective of increasing power densities and reducing losses. The behavior of a BSCCO bulk rotor has been tested in rotating magnetic fields produced by two poles and three phase motor coils fed by a PWM inverter at 77 K. To characterize the torque output capability of the HTS hysteresis motor, speed versus torque and current versus torque are tested. Experimental results for the HTS hysteresis motor are presented.**

Keywords— **HTS hysteresis motor, BSCCO**

I. Introduction

A VARIETY of electric power applications for high-T_c superconductor (HTS) have been proposed or are now in development. The electric power devices and components being designed to incorporate superconducting technology will operate more efficiently than their conventional alternatives. In conventional motors, currents flow in copper coils to generate magnetic fields. HTS can carry much larger electrical currents, which means a smaller and more powerful system. HTS bulks also give an excellent opportunity to elaborate a new type of HTS motor. There are now many attempts for preliminary development of HTS motors.

Such HTS motors could be classified into the following four types: the motor with HTS field windings [1], the trapped flux HTS motor which uses higher trapped field levels of HTS bulks than traditional permanent magnets [2], the reluctance motor with HTS blocks which work as concentrators of the magnetic flux along the d axis [3], and the hysteresis motor with cylindrical and disk HTS rotors [4].

Manuscript received September 18, 2000.
I. Muta is with the Graduate School of Engineering, Kyoto University, Yoshida-Honmachi, Sakyo-ku, Kyoto, 606-8051, Japan (telephone: +81-75-753-5292, e-mail: muta@kuee.kyoto-u.ac.jp).
Hun June Jung is with the Graduate School of Engineering, Kyoto University, Yoshida-Honmachi, Sakyo-ku, Kyoto, 606-8501, Japan (telephone: +81-75-753-5294, e-mail: hjjung@audrey.kuee.kyoto-u.ac.jp).
Tomohiro Hirata is with the Graduate School of Engineering, Kyoto University, Yoshida-Honmachi, Sakyo-ku, Kyoto, 606-8501, Japan (telephone: +81-75-753-5294, e-mail: hirata@audrey.kuee.kyoto-u.ac.jp).
Taketsune Nakamura is with the Graduate School of Engineering, Kyoto University, Yoshida-Honmachi, Sakyo-ku, Kyoto, 606-8501, Japan (telephone: +81-75-753-5294, e-mail: tk_naka@kuee.kyoto-u.ac.jp).
Tsutomu Hoshino is with the Graduate School of Engineering, Kyoto University, Yoshida-Honmachi, Sakyo-ku, Kyoto, 606-8501, Japan (telephone: +81-75-753-5293, e-mail: hoshino@asl.kuee.kyoto-u.ac.jp).
Takeshi Konishi is with the Railway Technical Research Institute, Tokyo, Japan (telephone: +81-952-28-8641, e-mail: takeshi@rtri.or.jp).

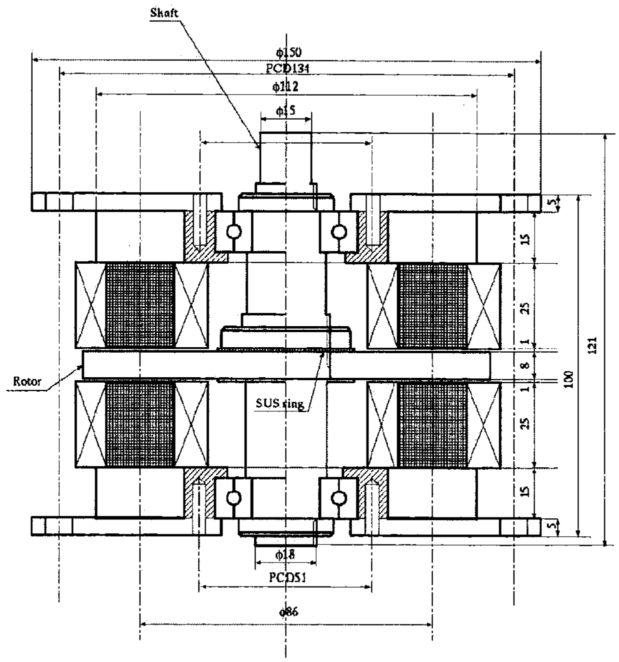

Fig. 1. Construction of the HTS hysteresis motor.

At the first stage of our studies on the HTS motors, we are aiming at academically investigating the torque generation mechanism and electromagnetic properties of YBCO and BSCCO. In further studies, we will incubate cryogenic engineering. Also, we will test and calculate the performance for the present motor.

In this paper, a small axial type HTS hysteresis motor immersed in liquid nitrogen is studied. Experimental results of torque vs. speed and torque vs. current characteristics are presented. Some problems of experiment and next study are discussed.

A general view of the HTS hysteresis motor is shown in Fig. 1. The HTS hysteresis motor is constructed such that the air gap length between the stator core and the disk is variable. Dimensions of the disk are also variable. The stator consists of laminated cores and twelve concentrated armature windings. For the armature winding, a coil wound with copper wire (0.8 mm in diameter) is used, and the number of turns of each winding is 25. Armature windings are wye connected and supplied electric current from a three-phase PWM inverter.

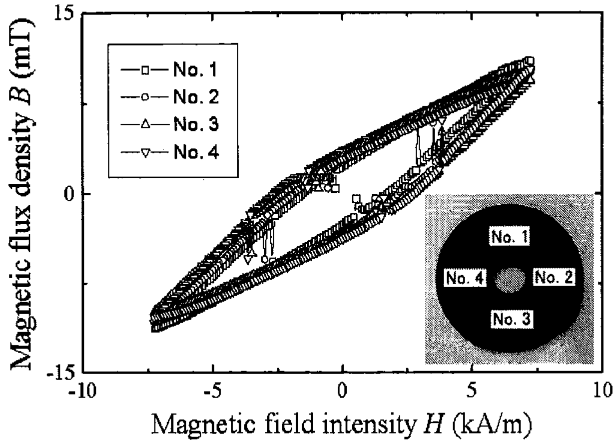

Fig. 2. Photograph and magnetic hysteresis curves (77.3K) of BSCCO-2223 bulk disk. Hysteresis curves are measured on different four points (see the photograph).

II. Magnetic Properties of BSCCO-2223 Disk

The magnetic properties of BSCCO-2223 disk used for the rotor are measured. This disk has 118.8 mm, 26.1 mm and 7.3 mm for outer diameter, inner diameter and height, respectively. The critical current density, J_c, and the critical temperature, T_c, are, respectively, 3×10^7 A/m^2 (77.3 K, self-field) and 105 K.

A photograph and magnetic hysteresis curves at 77.3 K of BSCCO-2223 bulk disk are shown in Fig. 2. The hysteresis curves are measured on four different points (see the photograph). To measure the magnetization of BSCCO-2223 disk, the armature round core and the armature winding used for the HTS hysteresis motor are used. They are placed perpendicular to the surface of the disk and the winding is connected to a power supply. A miniature Hall sensor is also placed on the surface of the disk and is used to measure the magnetic flux density of the disk. The apparatus is immersed in liquid nitrogen, and the magnetization measurement is performed with zero-field cooling.

To obtain a large torque from a hysteresis motor, it is desirable that a hysteresis loop covers as large area as possible [5]. Compared with conventional magnetic materials, HTS materials have a larger hysteresis loop, which increases the power density of a hysteresis motor.

As shown in Fig. 2, the magnetization has a slightly different hysteresis loop, depending upon the position of the measurement. The reason may be the poor crystal structure of BSCCO-2223 bulk. It should be noted that measuring the magnetization of BSCCO-2223 disk shown in Fig. 2 was carried out again on September 2000, and these magnetization curves are significantly different from ones obtained last November 1999 [6]. Degradation was observed.

III. Magnetic Field Distribution

Most electric machines, especially large machines, are designed so that the stator windings produce a relatively good approximation of sinusoidal air gap flux distribution so as to minimize harmonics. Because we used concentrated armature windings in this experiment, the radially directed flux density around the circumference of the air gap contains harmonic components. The amplitudes of the harmonics are listed in Table I. Also, the laboratory made HTS hysteresis motor does not have an uniform air gap, which produces more harmonic components. Such facts would have great influence on torque vs. speed curves, etc. of this machine, as described later.

TABLE I
Harmonic Components

Harmonics	Amplitude
1st	1.000
5th	0.754
7th	0.546
11th	0.109
13th	0.061

IV. Resistance and Inductance Tests

The phase resistance and inductance are measured using a multimeter. Unlike other synchronous motors, one can not measure the synchronous impedance of a hysteresis motor by a short circuit test, in which the motor is driven at synchronous speed with all three phases shorted together [7]. However, the short circuit current is given by a locked test. The synchronous impedance can be calculated using the short circuit current.

Using the resistance and inductance measurement results, an equivalent circuit can be built [8]. The HTS hysteresis motor is cooled by liquid nitrogen directly. It makes an additional loss due to the viscosity of liquid nitrogen. In the equivalent circuit, this loss has to be considered. The electrical equivalent circuit of the HTS hyteresis motor is shown in Fig. 3. The equivalent circuit has the following parameters: $r = 0.7\ \Omega$, $x = 1.0\ \Omega$, $r_{\mathrm{h}} = 0.579\ \Omega$, $x_{\mathrm{h}} = 18.6\ \Omega$ and $r_{\mathrm{v}} = 1.3\ \Omega$. During start-up a traditional hysteresis motor has both characteristics of induction motor and synchronous motor. Therefore, in the equivalent circuit, there are combined parameters with both functions. In Fig. 3, conventional impedance and reactance such as $(r + jx)$ of the winding exist, while r_{h} element corresponds to hysteresis loss. However, the $(1-s)r_{\mathrm{h}}$ element indicates the start-up torque occurence of an induction motor. Of course, when the motor is synchronized, slip s, equals 0, and so it serves as a synchronous motor. The above performance can be represented in the same equivalent circuit. Over all, compared to conventional hysteresis motors, the parameters of the equivalent circuit have almost the same meanings, but the value of r_{h} greatly depends on HTS bulk's characteristics. Generally speaking, r_{h} is larger because of HTS motor's big hysteresis loop.

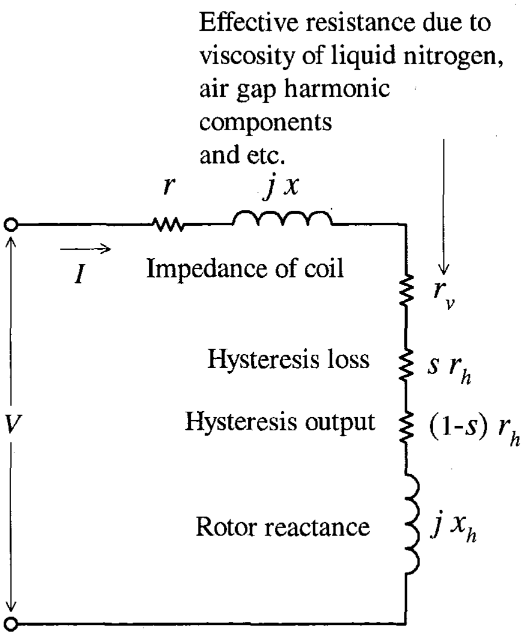

Fig. 3. Equivalent circuit of the HTS hysteresis motor per phase.

V. Torque vs. Speed and Torque vs. Current Characteristics

The torque measurement apparatus consist of a magnetic particle brake, torque/speed meter, and simple cryogenic system, consisting of an open metal Dewer. The HTS hysteresis motor under test is powered with a three-phase PWM inverter with a rated voltage of 200 V and a rated power of 1.5 kW.

Generally, hysteresis motors exhibit flat torque characteristics up to synchronous speed. It means the hysteresis loss, which produces torque, is independent of the field rotational frequency. If the field changing time is much greater than the fluxon transit time, then the fluxons can be assumed to move instantaneously, and the constant torque against speed characteristic is valid in HTS hysteresis motors [9].

The experimental result of torque vs. speed is shown in Fig. 4. As shown, the rotating speed of the HTS hysteresis motor does not exceed 400 rpm at 50 Hz, 2.0 A. The reason for this is as follows. The hysteresis disk is conductive, which produces eddy currents. It makes the HTS hysteresis motor operate as an induction motor with a slip greater than 0.75, and the concentrated winding causes torque reduction. Because of the concentrated winding, harmonic components are produced in the air gap. This causes the speed to decrease.

Fig. 5 shows the torque vs. current of the HTS hysteresis motor. The torque is dependent on the applied field. The torque varies with B^3 for small flux penetrations, changing over to a linear dependence for large penetrations [10]. The functional dependence of the torque on the applied current is obtained with least square fitted polynomial functions to

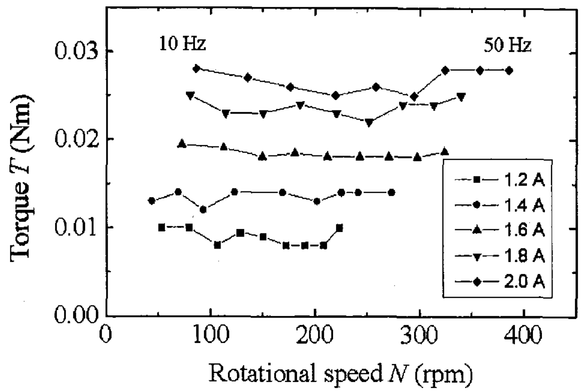

Fig. 4. Speed versus torque characteristics of the HTS hysteresis motor.

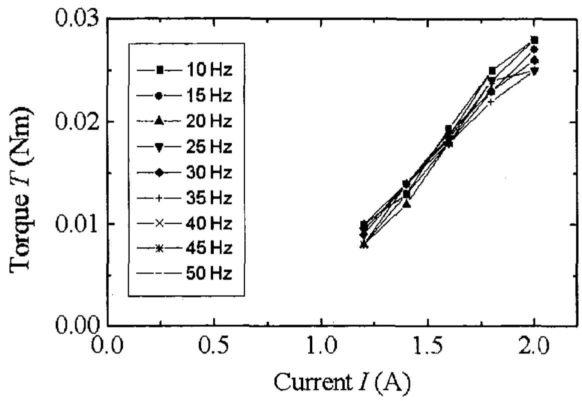

Fig. 5. Current versus torque characteristics of the HTS hysteresis motor.

I in the range $I \geq 1.2$ A. The current vs. torque is given as (1).

$$T = aI - b \qquad (I \geq 1.2\text{A}) \qquad (\text{Nm}) \qquad (1)$$

where, $a = 2.23 \times 10^{-2}$ NmA^{-1} and $b = 1.78 \times 10^{-2}$ Nm.

Torque is out of the range of the torquemeter in the range $I < 1.2$ A. However, we can suppose the torque is exponentially increasing in this range from the experimental results which are measured in the range of $I \geq 1.2$ A. We understand as follows from the experiment. For the current range of $0 \text{ A} < I < 1.2$ A, magnetic flux penetrates into the disk partially and the torque is small. For $I > 1.2$ A, however, magnetic flux penetrates into the disk globally and torque is increasing as current.

VI. Conclusion

Experimental results of the laboratory-made HTS hysteresis motor are unsatisfactory because of many elements that need to be improved in fabrication. Also, experimental methods have to be studied for precise performance evaluation of the HTS hysteresis motor. In this experiment, preliminary understanding has been obtained so as to proceed to the next study. In the next step, a new motor will

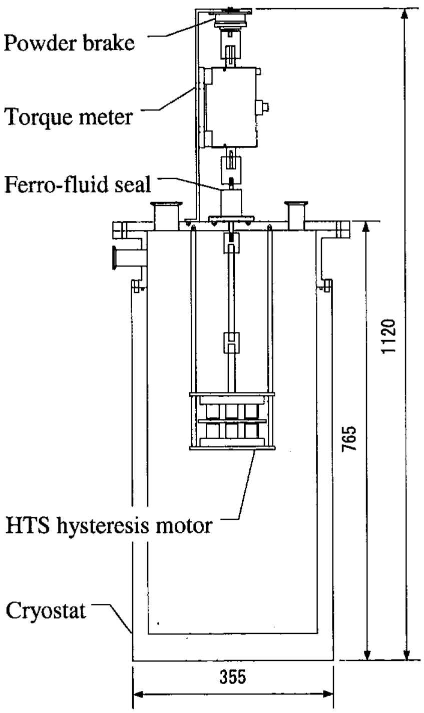

Fig. 6. New apparatus for the next experimental study.

be developed from the point of view of achieving sinusoidal rotating field, uniform air gap, and good crystal structure of HTS disk. HTS bulk motor is a good example to understand electrodynamics of HTS bulk, so we will study it more. A new experimental facility under construction is shown in Fig. 6. This facility has been improved to carry out various tests automatically with high accuracy and under many different conditions.

References

[1] J. D. Edick, R. F. Schiferl, and H. E. Jordan, "High temperature superconductivity applied to electric motors", *IEEE Trans. Appl. Superconduct.*, vol. 2, no. 4, pp. 189-194, Dec. 1992.

[2] A. D. Carpo and J. D. Lloyd, "Homopolar DC motor and trapped flux brushless DC motor using high temperature superconducting materials", *IEEE Trans. Magn.*, vol. 27, no. 2, pp. 2244-2247, Mar. 1991.

[3] L. K. Kovalev, K. V. Ilushin, V. T. Penkin, and K. L. Kovalev, "Hysteresis and reluctance electric machines with bulk HTS elements. Resent results and future development", *Supercond. Sci. Technol.*, vol. 13, pp. 498-502, 2000.

[4] M. D. McCulloch and D. Dew-Hughes, "Brushless AC machines with high temperature superconducting rotors", *Mater. Sci. Eng. B*, vol. 53, pp. 211-215, 1997.

[5] T. Kenjo, "Precision motors used in electronic equipment", Sogo Electronic Publishing Company, Tokyo, 1979 (In Japanese).

[6] I. Muta, T. Nakamura, T. Hirata, T. Hoshino and T. Konishi, "Preliminary study on axial type BSCCO superconducting motor", *ICMC 2000, Rio de Janeiro-RJ, Brazil*, SA145, Jun. 2000.

[7] J. R. Hendershot Jr., T. J. E. Miller, "Design of brushless permanent magnet motors", Oxford University Press, Oxford, 1994.

[8] S. Miyairi and T. Kataoka, "A basic equivalent circuit of the hysteresis motor", IEEJ, vol. 85, no. 925, pp. 1740-1748, Oct. 1965 (In Japanese).

[9] G. J. Barnes, D. Dew-Hughes, and M. D. McCulloch, "Finite difference modeling of bulk high temperature superconducting cylindrical hysteresis machines", *Supercond. Sci. Technol.*, vol. 13, pp. 229-236, 2000.

[10] R. V. Harrowell, "AC loss in rotating and reciprocating superconductors and normal superconductors", *J. Phys. D.:Appl. Phys.* , vol. 4, pp. 1769-1775, 1971.